Three-dimensional localized-delocalized Anderson transition in the time domain

Dominique Delande,[1] Luis Morales-Molina,[2] and Krzysztof Sacha[3,4]

[1] *Laboratoire Kastler Brossel, UPMC-Sorbonne Universités, CNRS, ENS-PSL Research University, Collège de France, 4 Place Jussieu, 75005 Paris, France*

[2] *Departamento de Física, Facultad de Física, Pontificia Universidad Católica de Chile, Casilla 306, Santiago 22, Chile*

[3] *Instytut Fizyki imienia Mariana Smoluchowskiego, Uniwersytet Jagielloński, ulica Profesora Stanisława Łojasiewicza 11, 30-348 Kraków, Poland*

[4] *Mark Kac Complex Systems Research Center, Uniwersytet Jagielloński, ulica Profesora Stanisława Łojasiewicza 11, 30-348 Kraków, Poland*

Systems which can spontaneously reveal periodic evolution are dubbed time crystals. This is in analogy with space crystals that display periodic behavior in configuration space. While space crystals are modelled with the help of space periodic potentials, crystalline phenomena in time can be modelled by periodically driven systems. Disorder in the periodic driving can lead to Anderson localization in time: the probability for detecting a system at a fixed point of configuration space becomes exponentially localized around a certain moment in time. We here show that a three-dimensional system exposed to a properly disordered pseudo-periodic driving may display a localized-delocalized Anderson transition in the time domain, in strong analogy with the usual three-dimensional Anderson transition in disordered systems. Such a transition could be experimentally observed with ultra-cold atomic gases.

PACS numbers: 71.30.+h, 05.30.Rt, 71.23.An, 67.85.-d

arXiv:1702.03591v1 [quant-ph] 12 Feb 2017

The fact that a detector, placed at some position, has a large probability to click at a certain moment in time when a particle is passing nearby is not very surprising. It is more interesting when this localisation has universal characteristics such as an exponential shape. This is the case when temporal Anderson localization is induced by a fluctuating driving force.

Usual Anderson localization is the configuration space exponential localization of eigenstates in the presence of a spatially disordered potential [1]. It is accompanied by the inhibition of transport due to destructive interference between different multiple scattering paths. Anderson localization may also take place in momentum space – where it is called "dynamical localization" – e.g. in the so-called kicked rotor, where an effective pseudo-disorder is induced by the classically chaotic dynamics [2–4].

The interference between paths scattered by a disorder depends on their geometrical properties and especially on the dimension of a system. According to the scaling theory of localization [5], one-dimensional (1D) and time-reversal invariant spinless 2D systems reveal localization regardless how weak the disorder is. In the 3D case, the situation is more complicated since the scaling theory predicts a second order phase transition — for a fixed disorder strength, all eigenstates of a system with energies up to the so-called mobility edge are localized and the other ones are not. How the mobility edge depends on the disorder has been analyzed in a variety of systems [6]. A rotor driven by a quasi-periodic sequence of kicks with d quasi-periods can be mapped on a d-dimensional pseudo-disordered system, allowing for a simple experimental method for studying Anderson localization in dimension d. This made it possible to investigate theoretically and experimentally the critical behavior in the vicinity of the 3D mobility edge [7, 8].

Anderson localization in the time domain can be realized in systems that are perturbed by a time fluctuating force, provided the latter is repeated periodically with a frequency that is resonant with the unperturbed motion of the system [9, 10]. In classical mechanics, the fluctuating force produces a diffusive motion. In the quantum description, interference effects cause the system to localize. That is, if we put a detector close to any point of the trajectory, we will observe that the detection probability is exponentially localized around a certain moment in time. Moreover, this exponential profile comes back every period of the classical motion. Thus, we deal with a situation analogous to Anderson localization of a particle on a ring (periodic boundary conditions) in the presence of a disordered time-independent potential. By traveling periodically around the ring, one observes periodically a localized density profile.

Anderson localization in time belongs to more general phenomena dubbed time crystals [11, 12]. Time crystals are systems that can spontaneously switch to a periodic motion. That is, even if they are prepared in an eigenstate, which possesses continuous time translational symmetry, a small perturbation can push them to periodic motion. There is a debate in the literature whether continuous time translational symmetry can be spontaneously broken [13–20]. So far it has been shown [21–26], and demonstrated experimentally [27, 28], that spontaneous breaking of a discrete time translational symmetry to another discrete one is possible. Here, we will not consider this problem of spontaneous formation of time crystals. We will model crystalline behavior by periodically driven systems, in analogy with condensed matter physics where spatially periodic potentials are used to

model space crystals.

Time is a single degree of freedom, therefore, we cannot expect multidimensional time crystals. In this Letter, we show that time crystal phenomena with properties of multidimensional condensed matter systems can be observed. More precisely we demonstrate the analog in the time domain of the usual three-dimensional localized-delocalized Anderson transition [6].

Let us consider a particle with a unit mass moving in the 3D space with periodic boundary conditions (3D torus) whose position is denoted by three angles: θ, ψ and ϕ. We assume that the particle is perturbed by a temporally disordered potential, i.e. the Hamiltonian of the system reads

$$H = \frac{p_\theta^2 + p_\psi^2 + p_\phi^2}{2} + V_0 g(\theta) g(\psi) g(\phi) f_1(t) f_2(t) f_3(t), \quad (1)$$

where V_0 is the amplitude of the perturbation. The time dependent functions are periodic but between t and $t + 2\pi/\omega_i$ they perform random fluctuations, i.e. $f_i(t+2\pi/\omega_i) = f_i(t) = \sum_{k\neq 0} f_k^{(i)} e^{ik\omega_i t}$ where $f_k^{(i)} = f_{-k}^{(i)*}$ are independent random numbers. We assume that the ratios of the frequencies ω_i are irrational numbers. In contrast, $g(x)$ is assumed to be a regular function — we choose $g(x) = x/\pi$ for $x \in [-\pi, \pi[$, i.e., $g(x) = \sum_n g_n e^{inx}$ where $g_n = \frac{i(-1)^n}{\pi n}$ for $n \neq 0$ and $g_0 = 0$. Thus, we deal with a perturbation which behaves regularly in the configuration space (for fixed time) but which is disordered in time. In the following we choose the $f_k^{(i)}$ components so that:

$$|g_k f_k^{(i)}| = \frac{1}{\sqrt{k_0}\pi^{1/4}} e^{-k^2/(2k_0^2)} \quad (2)$$

with k_0 a free-to-choose parameter and $\mathrm{Arg}(f_k^{(i)})$ (for $k > 0$) are independent random variables chosen uniformly in the interval $[0, 2\pi[$.

Let us switch to the moving frame where $\Theta = \theta - \omega_1 t$, $\Psi = \psi - \omega_2 t$ and $\Phi = \phi - \omega_3 t$. In this frame, Θ, Ψ and Φ are slowly varying variables if we choose the conjugate momenta $P_\Theta = p_\theta - \omega_1 \approx 0$, $P_\Psi = p_\psi - \omega_2 \approx 0$ and $P_\Phi = p_\phi - \omega_3 \approx 0$. In the secular approximation [29, 30], the dynamics of the slowly varying variables is described by an effective Hamiltonian obtained by averaging the original Hamiltonian over time:

$$H_{\mathrm{eff}} = \frac{P_\Theta^2 + P_\Psi^2 + P_\Phi^2}{2} + V_{\mathrm{eff}}(\Theta, \Psi, \Phi), \quad (3)$$

with $V_{\mathrm{eff}} = V_0 h_1(\Theta) h_2(\Psi) h_3(\Phi)$ where

$$h_i(x) = \sum_{k\neq 0} g_k f_{-k}^{(i)} e^{ikx}. \quad (4)$$

In Eq. (3), the constant term $(\omega_1^2 + \omega_2^2 + \omega_3^2)/2$ is omitted. To obtain H_{eff} we take advantage of the fact that the ratios of the frequencies ω_i are irrational numbers. The first order of the secular approximation (3) is valid provided the amplitude of the perturbation V_0 is small or ω_i's are large and fulfill the relations $\omega_1 > 2k_0\omega_2$ and $\omega_2 > 2k_0\omega_3$, i.e. the second order correction terms, $V_0^2/(\sum_i n_i\omega_i)^2 e^{-\sum_i n_i^2/4k_0^2}$, never suffer from a small denominator problem and are negligible.

The effective potential $V_{\mathrm{eff}}(\Theta, \Psi, \Phi)$ is a product of three independent disordered potentials h_i along each degree of freedom. It can be characterized by its two-point correlation function which is trivially factorized as a product of three times the same correlation function along the three directions. In the limit of relatively large k_0 we are interested in, there is a large number $\simeq k_0$ of random contributions in the sum (4); from the central limit theorem, we deduce that $h_i(x)$ has a Gaussian distribution with zero mean [31]. The correlation function is easily computed and, for large k_0, it reads

$$\overline{h_i(x')h_i(x'+x)} = V_0^2 \exp\left(-\frac{x^2}{2\sigma^2}\right), \quad (5)$$

where $\overline{\ }$ denotes the averaging over disorder realizations. $\sigma = \sqrt{2}/k_0$ is the correlation length of the disordered potential.

Let us assume, for a moment, that Θ, Φ and Ψ are not limited to the interval $[0, 2\pi[$ but extend from minus infinity to infinity. $V_{\mathrm{eff}}(\Theta, \Psi, \Phi)$ being a generic 3D random potential, one expects a localized-delocalized transition to take place at some value of the energy E_c called the mobility edge. There are three different energy scales in the problem: the strength V_0 of the potential, the energy E of the particle and the so-called correlation energy

$$E_\sigma = \frac{1}{\sigma^2} = \frac{k_0^2}{2}. \quad (6)$$

E_σ sets the natural energy scale of the problem [32], so that the ratio E_c/E_σ depends only on the ratio V_0/E_σ.

In 3D, the Anderson transition takes place in the regime of strong disorder, so that no analytic prediction is available and one has to resort to the indignity of numerical calculations in order to compute the position of the mobility edge as well as the localization length below it. We used the transfer matrix method described in [33]. To make a long story short, we discretize the configuration space on a (sufficiently dense) 3D rectangular grid and recursively compute the total transmission of a bar-shaped grid with length L and square transverse section $M \times M$, with $M \ll L$. This system can be viewed as quasi-1D and is thus Anderson localized: its total transmission decays like $\exp(-2L/\lambda_M)$ where λ_M is the quasi-1D localization length in units of the lattice spacing. In practice, the log of the total transmission is a self-averaging quantity which can be safely computed. λ_M depends on M, on the energy and on the disorder strength. Figure 1(a) shows the ratio λ_M/M as a function of energy, for various M values, at a fixed disorder strength $V_0 = E_\sigma$. At low energy, in the localized

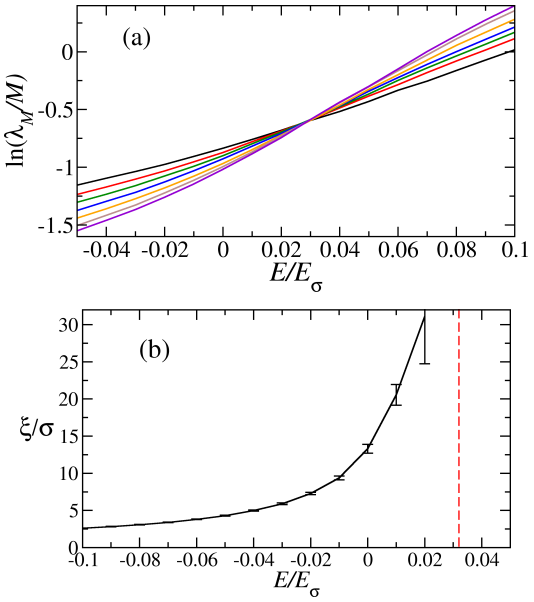

FIG. 1. (color online) Numerical determination of the mobility edge for $V_0 = E_\sigma$. For a given energy, we compute the localization length λ_M of a long bar-shaped grid with square section $M \times M$. (a): Each curve is computed for a single M value from 25 to 55 with step 5 (slope increases with M) and shows λ_M/M vs. energy. The various curves cross at the position of the mobility edge $E_c/E_\sigma = 0.032 \pm 0.002$. (b): The localization length ξ vs. energy, in the localized regime. It shows an algebraic divergence near the mobility edge, indicated by the red dashed line.

regime, λ_M/M decreases with M and eventually behaves like λ_∞/M, with $\lambda_\infty = \lim_{M\to\infty} \lambda_M$ the 3D localization length. In contrast, at high energy, λ_M/M increases with M, a signature of the diffusive regime. At the mobility edge, λ_M/M is a constant Λ_c of order unity, meaning that the quasi-1D localization length is comparable to the transverse size of the system, a signature of marginal 3D localization. Thus, the mobility edge can be obtained by looking at the point where all curves cross in Fig. 1(a), near $E_c/E_\sigma = 0.03$. In order to pinpoint more accurately the position of the mobility edge, we use a finite-size scaling analysis [33, 34] which gives $E_c/E_\sigma = 0.032 \pm 0.002$. It also makes it possible to compute the 3D localization length below the mobility edge, shown in Fig. 1(b).

Coming back to the initial time-dependent driven Hamiltonian (1), observing a temporal dependence with time crystal properties requires to have a periodic motion localized along the 3 directions, that is a stationary eigenstate of the effective Hamiltonian (3) with a localization length much smaller than the spatial period 2π. By inspecting the results in Fig.1(b), we chose an exemplary value $\sigma = 0.1$ (corresponding to $k_0 = 10\sqrt{2}$). At energy $E = -0.05E_\sigma$, the localization length is predicted to be $\xi \approx 4.3\sigma = 0.43$, sufficiently smaller than 2π to observe good localization properties. We numerically diagonalized the Hamiltonian (3) discretized on a 100x100x100 grid using the JADAMILU package [35] to obtain few eigenstates with energy close to $-0.05E_\sigma$. The localization properties of a typical eigenstate are shown in Figure 2. As expected, they display an overall exponential localization with the expected localization length and with the large fluctuations typical of eigenstates. The lower plots show how the probability density for detecting a particle at a fixed point in the configuration space changes as time evolves. It changes periodically with the maximum value roughly 5 orders of magnitude larger than the minimum, i.e. it behaves like the probability in the case of Anderson localization in a space crystal with periodic boundary conditions. Other eigenstates, either at slightly different energy and/or for a different disorder realization, have similar localization properties.

Finally, let us analyze a possible experimental realization of Anderson localization in the time domain with ultra-cold atomic gases. We will focus on the simplest version when a single frequency driving is applied and only one spatial degree of freedom is involved. In order to realize a system described by the Hamiltonian $H = p^2/2m + V_0 g(2\pi z/L_z) f_1(t)$, which is analogous to (1), we can use a sawtooth shape periodic potential along the z direction with spatial period L_z [36, 37]. Initially, an ultra-cold atomic cloud should be prepared in a shallow trap and in the presence of a strong optical lattice along the z axis which has to be periodic with period L_z but can have an arbitrary shape. This creates a series of independent slices of the atomic cloud which consist of well defined numbers of atoms but do not have any mutual phase coherence, see Fig. 3(c). Next, the initial optical lattice and the shallow trapping potentials are turned off while the sawtooth potential temporally modulated by the $f_1(t)$ function, is turned on. At the same moment, the scattering length of atoms is adjusted to zero by means of a Feshbach resonance and atoms are kicked so that their average momentum along the z direction is $\langle p \rangle = \omega_1 m L_z/2\pi$, see Fig. 3(d). If these conditions are met, the effective Hamiltonian, in the frame moving with the velocity $\omega_1 L_z/2\pi$, reads $H_{\rm eff} = P^2/2m + V_0 \sum_k g_k f^{(1)}_{-k} e^{ik2\pi z/L_z}$ and Anderson localization along the z direction can be expected. This requires the localization length $\xi(E)$ corresponding to $E = \langle p_0^2 \rangle/2m$ to be smaller than L_z where $\langle p_0^2 \rangle$ is the initial dispersion of momenta of atoms along the z axis in the presence of the strong optical lattice potential at the beginning of the experiment. An example of experimental parameters is given in Fig. 3. It is not necessary to create an exact sawtooth periodic potential. For time modulation $f_1(t)$ consisting of, e.g., three harmonics ($k_0 = 3$), only the first three spatial harmonics of the sawtooth potential have to be reproduced. The presence of Anderson localization in time will have remarkable signatures in the described experiment. That is, after the turning off the initial optical lattice and trapping potentials, atoms expand slowly in the transverse directions

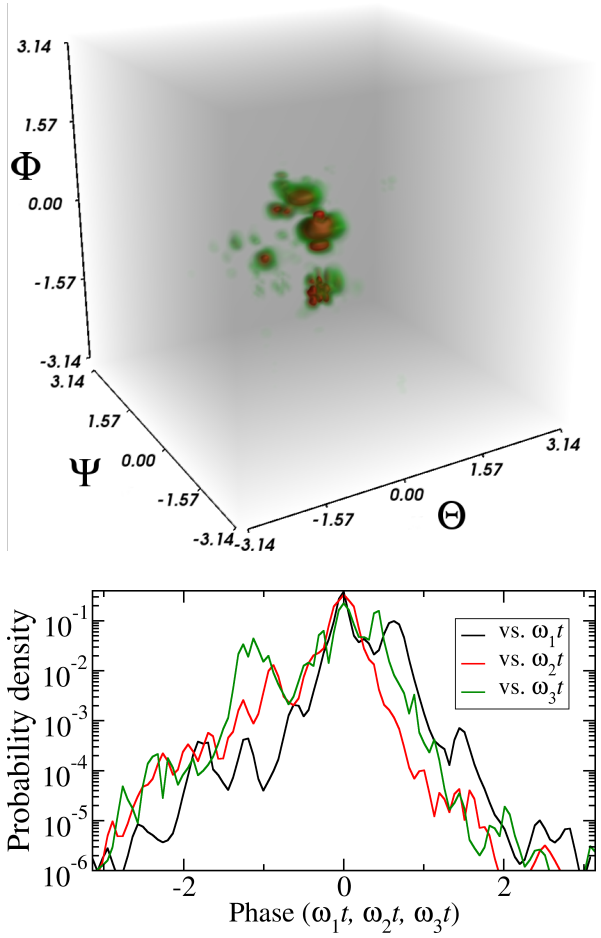

FIG. 2. (color online) Spatial probability density for a typical localized eigenstate of Hamiltonian (3) with correlation length of the disorder $\sigma = 0.1$, for $V_0 = E_\sigma$ and energy $E/E_\sigma = -0.049968$. The upper color 3D plot shows the disordered yet localized character of the state below the mobility edge. Lower plots show how probability densities at a fixed position in θ, ϕ or ψ in the laboratory frame (integrated along two remaining directions) evolve in time. The semi-logarithmic scale indicates an approximate exponential localization. In the rotating frame, the localization length $\simeq 0.4 = 4\sigma$ is in good agreement with the prediction of the transfer matrix calculation, $\xi = 4.3\sigma$ in Fig. 1. It implies that in the laboratory frame the localization length in time reads, e.g., $4\sigma/\omega_1$ if the probability density is integrated over ψ and ϕ.

but the width of the slices along the z direction remains smaller than L_z despite the fact that atoms fly over the time modulated sawtooth potential.

In conclusion, we have shown that, using a properly disordered, but pseudo-periodic, temporal driving of a 3D system, one can induce a non-trivial Anderson localization in the time domain and the localized-delocalized Anderson transition. This could be observed – in particular, but not exclusively, using cold atoms – through the existence of periodically evolving localized wavepackets displaying properties similar to those of space crystals

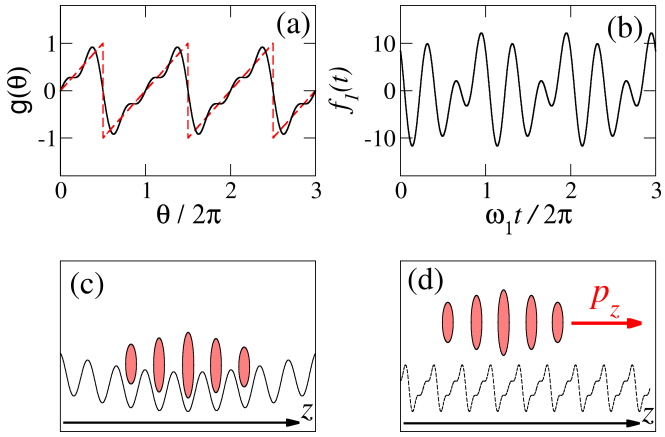

FIG. 3. Experimental proposal. (a) The red dashed line shows the shape of a sawtooth potential while the black solid line its approximation built with the first three spatial harmonics only. The latter can be created by means of an optical standing wave with wavelength λ and its first two harmonics. (b) Temporal modulation function $f_1(t)$ that consists of three harmonics with random phases and with the amplitude $|g_k f_k^{(1)}| = \frac{1}{\sqrt{k_0}}$ for $|k| \leq k_0 = 3$. (c) Schematic plot of the initial stage of the experiment: ultra-cold bosonic atoms are prepared in a strong optical lattice and shallow trapping potentials. We assume that for the amplitude of the lattice potential of the order of $30E_{\rm rec}$ (atomic recoil energy), slices of the atomic cloud are formed that consist of well defined numbers of particles and do not have mutual phase coherence. The average kinetic energy along the z direction is $\langle p_0^2\rangle/2m \approx 2E_{\rm rec}$. (d) Final stage of the experiment: for a perturbation amplitude $V_0 = 40E_{\rm rec}$, atoms accelerated to the average momentum $\langle p\rangle = m\omega_1\lambda/4\pi$ will fly over the time modulated sawtooth potential and do not spread along z due to the predicted Anderson localization. The predictions are valid provided $\omega_1 \geq 400E_{\rm rec}/\hbar$.

with disorder and with periodic boundary conditions but in the time domain.

This work was performed within the Polish-French bilateral POLONIUM Grant 33162XA and the FOCUS action of Faculty of Physics, Astronomy and Applied Computer Science of Jagiellonian University. We thank the authors of the Jadamilu library [35] that we used for large scale diagonalizations. This work was granted access to the HPC resources of TGCC under the allocations 2016-057644 and A0020507644 made by GENCI (Grand Equipement National de Calcul Intensif) and to the HPC resources of MesoPSL financed by the Region Ile de France and the project Equip@Meso (reference ANR-10-EQPX-29-01) of the programme Investissements d'Avenir supervised by the Agence Nationale pour la Recherche. Support of the National Science Centre, Poland via project No.2016/21/B/ST2/01095 (KS) is acknowledged.

[1] P. W. Anderson, Phys. Rev. **109**, 1492 (1958).

[2] F. L. Moore, J. C. Robinson, C. F. Bharucha, B. Sundaram, and M. G. Raizen, Phys. Rev. Lett. **75**, 4598 (1995).

[3] S. Fishman, D. R. Grempel, and R. E. Prange, Phys. Rev. Lett. **49**, 509 (1982).

[4] G. Casati, I. Guarneri, and D. L. Shepelyansky, Phys. Rev. Lett. **62**, 345 (1989).

[5] E. Abrahams, P. W. Anderson, D. C. Licciardello, and T. V. Ramakrishnan, Phys. Rev. Lett. **42**, 673 (1979).

[6] C. A. Müller and D. Delande, "Disorder and interference: localization phenomena," in *Lecture Notes of the Les Houches Summer School in Singapore: Ultracold Gases and Quantum Information*, Vol. 91 (Oxford Scholarship, 2011) Chap. 9, arXiv:1005.0915.

[7] G. Lemarié, J. Chabé, P. Szriftgiser, J. C. Garreau, B. Grémaud, and D. Delande, Phys. Rev. A **80**, 043626 (2009), arXiv:0907.3411 [quant-ph].

[8] I. Manai, J.-F. Clément, R. Chicireanu, C. Hainaut, J. C. Garreau, P. Szriftgiser, and D. Delande, Phys. Rev. Lett. **115**, 240603 (2015).

[9] K. Sacha, Sci. Rep. **5**, 10787 (2015).

[10] K. Sacha and D. Delande, Phys. Rev. A **94**, 023633 (2016).

[11] F. Wilczek, Phys. Rev. Lett. **109**, 160401 (2012).

[12] T. Li, Z.-X. Gong, Z.-Q. Yin, H. T. Quan, X. Yin, P. Zhang, L.-M. Duan, and X. Zhang, Phys. Rev. Lett. **109**, 163001 (2012).

[13] M. N. Chernodub, Phys. Rev. D **87**, 025021 (2013).

[14] F. Wilczek, Phys. Rev. Lett. **111**, 250402 (2013).

[15] P. Bruno, Phys. Rev. Lett. **110**, 118901 (2013).

[16] F. Wilczek, Phys. Rev. Lett. **110**, 118902 (2013).

[17] P. Bruno, Phys. Rev. Lett. **111**, 029301 (2013).

[18] T. Li, Z.-X. Gong, Z.-Q. Yin, H. T. Quan, X. Yin, P. Zhang, L.-M. Duan, and X. Zhang, (2012), arXiv:1212.6959.

[19] P. Bruno, Phys. Rev. Lett. **111**, 070402 (2013).

[20] H. Watanabe and M. Oshikawa, Phys. Rev. Lett. **114**, 251603 (2015).

[21] K. Sacha, Phys. Rev. A **91**, 033617 (2015).

[22] V. Khemani, A. Lazarides, R. Moessner, and S. L. Sondhi, Phys. Rev. Lett. **116**, 250401 (2016).

[23] D. V. Else, B. Bauer, and C. Nayak, Phys. Rev. Lett. **117**, 090402 (2016).

[24] C. von Keyserlingk, V. Khemani, and S. Sondhi, Phys. Rev. B **94**, 085112 (2016).

[25] N. Y. Yao, A. C. Potter, I. D. Potirniche, and A. Vishwanath, Phys. Rev. Lett. **118**, 030401 (2017).

[26] S. A. Weidinger, and M. Knap, arXiv:1609.09089.

[27] J. Zhang, P. W. Hess, A. Kyprianidis, P. Becker, A. Lee, J. Smith, G. Pagano, I.-D. Potirniche, A. C. Potter, A. Vishwanath, N. Y. Yao, C. Monroe, arXiv:1609.08684.

[28] S. Choi, J. Choi, R. Landig, G. Kucsko, H. Zhou, J. Isoya, F. Jelezko, S. Onoda, H. Sumiya, V. Khemani, C. von Keyserlingk, N. Y. Yao, E. Demler, M. D. Lukin, arXiv:1610.08057.

[29] A. Buchleitner, D. Delande, and J. Zakrzewski, Physics reports **368**, 409 (2002).

[30] A. J. Lichtenberg and M. A. Lieberman, *Regular and Stochastic Motion*, Applied Mathematical Sciences Vol. 38, edited by F. John *et al.* (Springer, Berlin 1983).

[31] When k_0 is not very large, there are some deviations from the formula given in the text. This may induce a small shift of the mobility edge, but the general picture is not affected.

[32] R. C. Kuhn, O. Sigwarth, C. Miniatura, D. Delande, and C. A. Müller, New J. Phys. **9**, 161 (2007).

[33] D. Delande and G. Orso, Phys. Rev. Lett. **113**, 060601 (2014).

[34] K. Slevin and T. Ohtsuki, New J. Phys. **16**, 015012 (2014).

[35] M. Bollhöfer and Y. Natay, Computer Physics Communications **177**, 951 (2007).

[36] S. Denisov, L. Morales-Molina, S. Flach, and P. Hänggi Phys. Rev. A **75**, 063424 (2007).

[37] T. Salger, S. Kling, T. Hecking, C. Geckeler, L. Morales-Molina, M. Weitz, Science 326, 1241 (2009).